FRACTURE ANALYSIS OF CONCRETE: A STEREOLOGICAL APPROACH

K. M. Nemati
Department of Civil and Environmental Engineering, University of California at Berkeley, Berkeley, California, U.S.A.

P. Stroeven
Faculty of Civil Engineering and Geosciences, Delft University of Technology, The Netherlands.

Abstract
This investigation examined a number of concrete specimens that were subjected to a variety of loading regimes for the purpose of studying stress-induced microcracking in concrete. A special technique using Wood's metal was developed that preserves the stress-induced microcracks in concrete as they exist under load. Scanning electron microscopy was used to capture images from the cross sections of the specimens. Next, stereology, a method that estimates the geometric statistical background for relating three-dimensional structures to their two-dimensional sections, was applied to obtain the total crack extension per unit of volume. Furthermore, 2-D features of the cracks were analyzed in the section plane, such as orientation, distribution and length.
Key words: Concrete, stereology, stress-induced microcracking, scanning electron microscopy, image analysis.

1 Introduction

Concrete, a heterogeneous, multiphase material, is a mixture of cement paste and fine and coarse aggregates of various sizes and shapes. In

terms of its mechanical behavior, concrete is often considered to be a three-phase composite structure: aggregate particles, the cement paste matrix in which they are dispersed, and the interfacial transition zones around the aggregate particles.

Since the 1920s researchers have assumed the existence of defects in concrete, called microcracks, but it wasn't until the early 1960s that the technology was developed to observe, measure, and characterize the mechanism of microcracking. The development of nonlinear fracture mechanics models in the 1970s and 1980s enabled the structure and behavior of concrete to be accurately modeled, and additional research in the 1980s and 1990s led to the application of fracture mechanics in the design of beams, anchorage, and large dams. Despite these advances, however, the theory of fracture mechanics was limited partly because of the poor understanding of the formation and propagation of microcracks in concrete. Attempts to analyze damage evolution using stereological techniques were conducted in the 1970s (Stroeven 1973, 1976, 1979), and such studies were able to reveal mechanisms of damage evolution in complicated loading cases, such as in the low-cycle fatigue domain (Reinhardt et al. 1978). By application of the fractal concept, recently the influence could be assessed of the sensitivity of the quantitative image analysis of microcracking in concrete on the spatial morphological features (Stroeven 1991, Carpinteri et al., 1997).

2 Methods for studying microcracking

The investigation of microcracking ranges from a macroscopic study of the behavior of cracked specimens to a microscopic study of the cracks themselves. The presence of microcracks was predicted on the basis of macrobehavior and verified by microscopic studies. Several methods have been used to study the microcracking of concrete: acoustic emission, sonic testing, dye techniques, microscopic techniques with dyes, the hydrophilic tracer liquid technique, mercury intrusion porosimetry, x-rays, optical and electron microscopy computerized tomography analysis, holographic interferometry, and the fluorescent spraying technique (Stroeven 1973, 1979). Some of these techniques are limited in their resolution, their sensitivity in detecting cracks, or their ability to make observations over a large area. Other methods do not allow for examination of the specimen under load or the require special preparation of the specimen, which alters its behavior.

The method described here involves the application of metal in the liquid phase, Wood's metal, to a concrete specimen; the special characteristics of Wood's metal preserves stress-induced microcracks in concrete, allowing for the detailed observation of microcracks in concrete

under load. Wood's metal has been used in the past few years to measure contact areas and voids between the surfaces of natural fractures, to measure the fracture of rocks, to fill voids and microcracks in clastic rocks specimens during loading, then solidifying it before unloading to preserve the microstructure in specimens under load, and to study the generation and interactions of compressive stress- induced microcracks in concrete (Nemati et al. 1998).

Wood's metal is a fusible alloy that is solid at room temperature, with a melting range from 71°C to 88°C. It has a Young's modulus of 9.7 GPa, a density of 9.4 g/cm^3, and does not change volume during hardening. In the liquid phase is it nonwetting, with an effective surface tension of about 400 mN/m, and can penetrate into flat cracks with apertures as fine as 0.08 microns under a pore pressure of 10 MPa. The advantage of such an alloy is that it can be intruded into voids and stress-induced microcracks while the specimen is held at the desired stress level and then solidified to preserve the geometry of the microcracks. This technique also avoids the problem of crack formation during specimen preparation. Using in conjunction with Scanning Electron Microscopy (SEM) with Backscattered Electrons (BSE), it allows the detailed observation of microcracks in concrete as they exist under load (the latter depends on the existence of pre-loading cracks, which are open under load).

In this test series all specimens were subjected to a compressive loading of about 80- 85% of their ultimate strength, and the SEM was operated at 15 kV and a probe of current of around 1 nA at a working distance of 15 mm. The images were acquired by the image analyzer at a magnification of x60 and digitized into an array of 512x512 pixels, with 256 gray levels (1 pixel = 3.3 μm). A typical BSE image is given in Fig. 1. Figure 2 shows a histogram of the distribution of grey levels in the BSE image superimposed on the original image. As the average atomic number of the Wood's metal is much higher than those of the cement paste and the aggregates, impregnated cracks and pores can be easily distinguished in the BSE image. The peak at the right (the high gray level) corresponds to the areas of Wood's metal, while the peaks to the left correspond to the cementitious phases and aggregates. This histogram was selected as the threshold value for discriminating the areas of Wood's metal. As shown in Fig. 3, the resulting image included small isolated pores, which were eliminated by applying a minimum-size threshold (scrap) for objects of 10 pixels (minimum feature size of approximately 33 μm).

Next, a skeletonized binary image was obtained by binary thinning. For every thinning step, pixels that were not relevant to the connectivity of an object were removed from the object margins, i.e., converted into background pixels, thus connectivity of objects was maintained. This

process was continued until all objects were reduced to a width of one pixel that approximates the skeleton. Figure 4 show the final binary image used for stereological measurements.
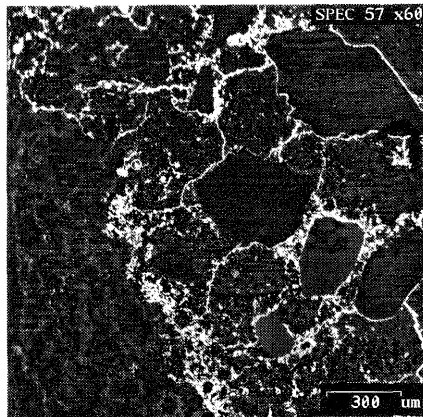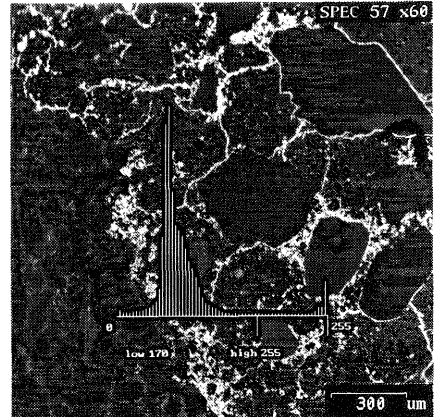

Fig. 1: A typical BSE image

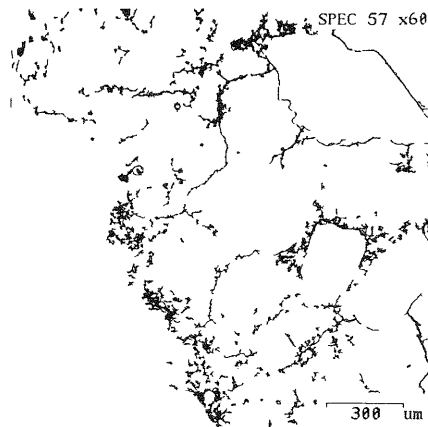**Fig. 2:** The gray level histogram

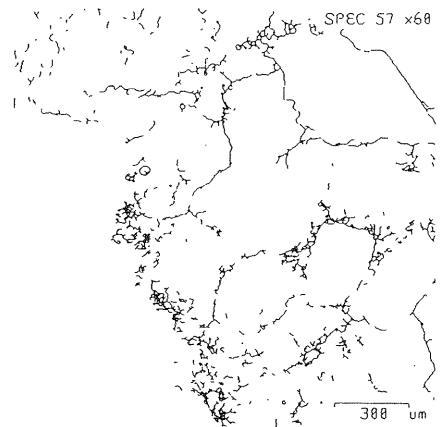**Fig. 3:** Thresholded image

Fig. 4: Binary-thinned image of the crack network in concrete

3 Stereology

All matter can be described in terms of zero, one, two, and three dimensions. Stereology interprets three-dimensional structures by means of their two-dimensional sections or projections. In a way stereology is the opposite of photogrammetry, which uses three- dimensional images in order to construct flat maps. Stereology techniques are often used for studying the three-dimensional structure of materials, particularly in other

material sciences. Stereology encompasses numerical characterizations of geometrical aspects of those features of the microstructure under study, like microcracks in concrete. In its broadest context, stereology includes all aspects of the methodology for the quantitative study of spatial structures, i.e., the design of experiments, the sampling strategy, the pattern of recognition and quantitative image analysis operations, the geometrical statistical theoretical framework for three-dimensional estimation of spatial parameters and their accuracy, and the qualitative interpretation of the outcomes.

There are various stereological strategies for solving spatial problems, depending on the objects of interest. This can be the analysis of the internal structure of single objects via a serial sectioning approach, which requires a deterministic strategy for three-dimensional construction. In materials science, however, stereology is used to assess the global spatial parameters of a dispersed "particulate" phase. Note that "particulate" can be interpreted in terms of aggregate particles of macroscopic dimensions or of cement particles on a microlevel. Pores or other defects are obtained upon taking zero phase stiffness. In cases of dispersed elements like cracks in the material body, stereological approaches are based on statistico-geometrical methods, sometimes encompassing a large number of two-dimensional images. This is the approach used in this study.

Reliable prediction of three-dimensional features of the structure of interest, in this case crack in a loaded specimen, can only be achieved when based on a representative sample. In general, this implies a sample of random sections or projections of sufficient extent. Basically, the quality of the prediction is inversely proportional to the square root of the effort, therefore by taking the sample four times larger will improve the quality of the estimate by a factor of two. In exceptional cases the structure itself consists of randomly dispersed elements. In such cases a single section, if extensive enough to contain a statistically significant number of features, will suffice to obtain valid results. Fundamental expressions have been determined that relate measurements on two-dimensional sections to the three-dimensional structure. Table 1 presents the terminology used here.

The relationships between L_A and S_V with P_L are presented below (Underwood, 1968). (Crack) surface area per unit volume, S_V:

$$S_V = 2P_L \quad \mu m^2 / \mu m^3 \tag{1}$$

(Crack) length per unit area, L_A:

$$L_A = \left(\frac{\pi}{2}\right) P_L \quad \mu m / \mu m^2 \tag{2}$$

and combined

$$\frac{\pi}{2} P_L = L_A = \frac{\pi}{4} S_V \tag{3}$$

51

Table 1. List of basic stereological symbols and their definition

Symbol	Dimensions	Definition
P_L	μm^{-1}	Number of intersections per unit grid line length between features (i.e. cracks) in the section plane, and a superimposed randomly oriented system of parallel lines.
$P_L(\theta)$	μm^{-1}	Ibid, but with the line array oriented at an angle θ to a reference axis.
L_A	$\mu m/\mu m^2$	Total crack length in a section per unit of area
S_V	$\mu m^2/\mu m^3$	Total crack surface area per unit of volume

4 Application of stereology to concrete fracture

Stroeven (1973, 1976, 1992), Ringot (1988), and Massat et al. (1988) successfully applied the concept of stereology to study micromechanical aspects of concrete. Whereas in the past this was not possible using manual methods, modern image analysis performs stereological analysis on a great number of images accurately and expeditiously.

The present investigation studied concrete cylinders tested in compression with various degrees of lateral confinement. The specimens while under load were impregnated with Wood's metal to preserve the pre-loading cracks and the stress-induced cracks. After the metal solidified, sections were cut from the specimens and examined using SEM. Image analysis and stereology were used to characterize the three-dimensional extent of the cracking, to determine the geometry (shape) of the stress-induced two-dimensional microcracks as they exist under load, and to assess the dependence of these damage parameters on the type of concrete and on the loading confinement.

The BSE images obtained using SEM (see Fig. 1) were analyzed using a Kontron image analyzer. Computer programs were developed to analyze the images based on the concept of stereology. The binary image (Fig. 4) was then intersected by an array of straight parallel lines at successively increasing angles of 0°, 15°, 30°, 45°, 60°, 75°, 90°, 105°, 120°, 135°, 150°, and 165° (shown in Fig. 5). The number of crack intersections at a given angle, θ, was then determined. Table 2 summarizes the results of the stereological analysis.
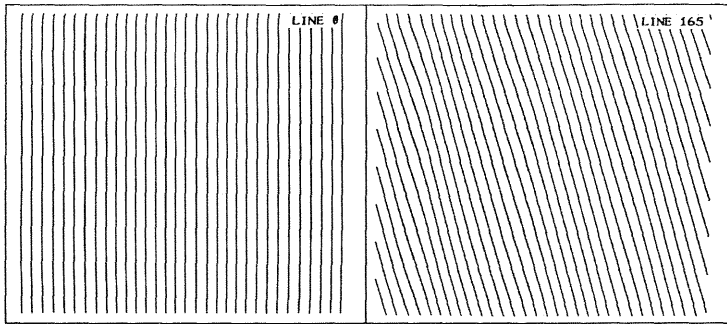
Fig. 5: Array of straight parallel lines

Table 2. Data from stereological analysis

SPECIMEN	AREA	% AREA	0	15	30	45	60	75	90	105	120	135	150	165	180	TOTAL	S_V
No Load	5228	0.98	21	20	19	16	18	20	19	19	18	16	18	20	21	226	7.0E-4
Uniaxial	10829	1.90	43	43	39	35	38	41	39	40	36	34	39	43	43	470	1.5E-3
Confined	6274	1.21	25	25	23	20	22	23	22	22	21	19	23	25	25	269	8.3E-4

Fig. 6 is a flow chart summarizing the computer program for stereological analysis.
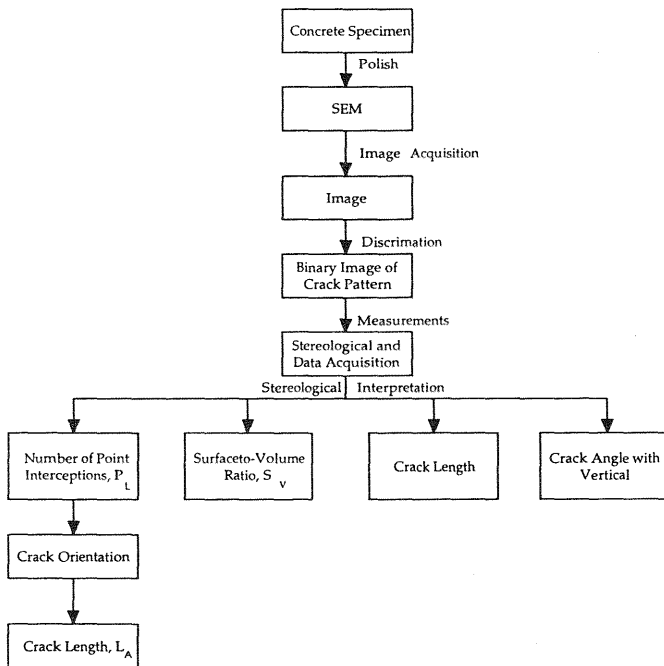

Fig. 6:
Flow chart for
stereological steps

4.1 Orientation of microcracks

A plot of the number of intersections of the line array with the network of thinned cracks for successive orientations of the grid is shown in Fig. 7.
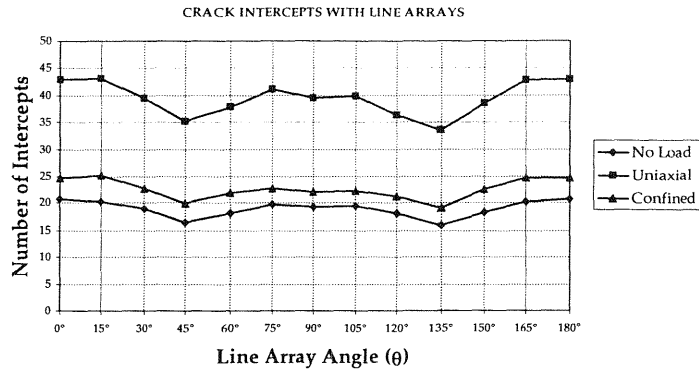
53

CRACK INTERCEPTS WITH LINE ARRAYS

Fig. 7: Areal crack orientation distribution

The figure demonstrates that on a microscopic scale, the cracking is relatively isotropic. The uniaxial section shows some tendency for a higher number of intersections for line arrays oriented parallel to the stress axis, indicating that the cracks in this section tended to run perpendicular to the loading direction; however, this tendency is not present in sections of the confined specimens.

Any tendency to anisotropy and anisometry in the underlying damage structure is due to the non-hydrostatic character of the loading. The heterogeneity of concrete greatly affects the mechanism of damage evolution on the microlevel. The relatively stiff and strong particles play an important role in normal concretes, particularly because of their relatively poor bond to the surrounding matrix. Upon visual examination, clearly a large proportion of the cracks occur at the cement paste-aggregate interfaces, as reported earlier. Although these interfaces are randomly oriented, cracking in the virgin state will never be random, therefore, the starting point of any mechanical test involves testing concretes with a partially ordered defect structure. Whether this is significant depends on the goals of the investigation. To a far lesser extent the same holds for the non-random influence of non-hydrostatic loadings on damage evolution. Total crack surface area per unit volume--seen as a relevant global three-dimensional damage evolution parameter--could be assessed with sufficient arrays for specific purposes, i.e., when comparing the influence of significantly different loading regimes.

4.2 Crack surface area, S_v

The stereological measurement of the surface-to-volume ratio, S_v (S/V), was determined from the basic equation for obtaining the total crack surface-area-per-unit-volume. Plots of S_v as a function of confinement is presented in Fig. 8. Crack surface area, S_v, decreases as the confining stresses increase.
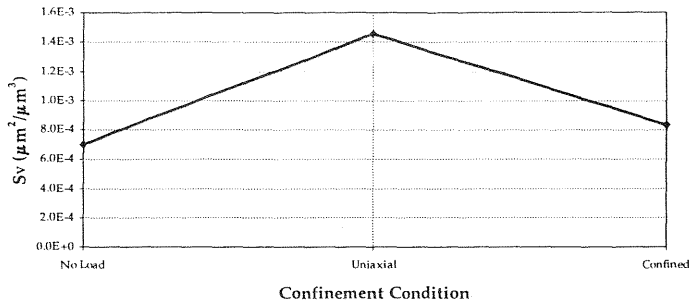
Fig. 8: Crack surface area (S_V) as a function of confinement

4.3 Crack length distribution

Based on stereological analysis, the total crack length-per-unit-area, L_A, also decreases with increasing confining stresses. Figure 9 shows the relationship between L_A and confinement conditions.
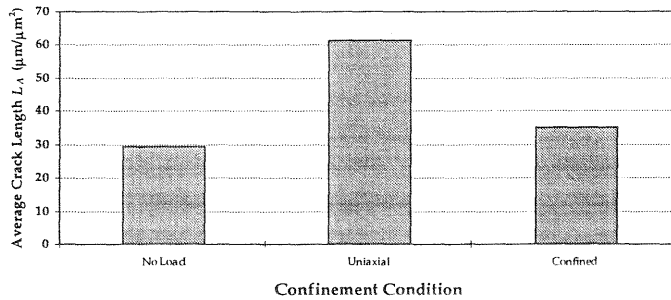

Fig. 9: Stereological measurement of total crack length per unit of area as a function of confinement

5 Summary and Conclusion

In this study, concrete specimens were subjected to compressive loading and microcracks were generated using several different mechanisms. The microcracks were generally with 15° of the direction of maximum compression. The concept of stereology, which interprets three-dimensional structures by means of their two-dimensional sections, was used to analyze images of these concrete specimens when subjected to different load regimes. The stereological prediction of the total surface area per unit volume of the cracks was found to be strongly influenced by the confining stress. Application of the confining stress resulted in a decrease in crack surface density, because the stress intensity factor is a

key component governing the stress field near the crack tip. The propagation of microcracks, controlled by the stress intensity factor at the microcrack tips, results from both local tensions, which generate the microcracks, and the overall field stress. The confining stress, which is orthogonal to the direction of maximum compression, adds a negative stress intensity factor, inhibiting further propagation of the microcracks.

6 References

Carpinteri, A., Chiaia, B., and Nemati, K. M. (1997). "Complex Fracture Energy Dissipation in Concrete Under Different Loading Conditions," **Mechanics of Materials**, 26(2): 93-108.

Massat, M., Ollivier, E., and Ringot, E. (1988). "Microscopic Analysis of Microcracking Damage in Concrete and Durability," **Lab. Materiaux et Durabilite des Constructions** (INSA-UPS), Toulouse, France.

Nemati, K.M., Monteiro, P.J.M., and Cook, N.G.W. (1998) "A New Method for Studying Stress-Induced Microcracks in Concrete," ASCE, **Journal of Materials in Civil Engineering**, 10(3).

Reinhardt, H.W., Stroeven, P., et al. (1978). "Einflusz von Schwingbreite, Belastungshöhe und Frequenz auf die Schwingfestigkeit vpn Beton bei niedrigen Bruchlastwechselzahlen," **Betonwerk+Fertigteil-Technik**, 44: 498-503

Ringot, E. (1988). "Automatic Quantification of Microcracks Network by Stereological Method of Total Projections in Mortars and Concretes," **Cement and Concrete Research**, 18: 35–43.

Stroeven, P. (1973). "Some Aspects of Micromechanics of Concrete," **Ph.D. Thesis**, Stevin Laboratory, Technological University of Delft.

Stroeven, P. (1976). "Application of Various Stereological Methods to the Study of the Grain and the Crack Structure of Concrete," **Journal of Microscopy**, 107(3):313–321.

Stroeven, P. (1979). "Geometric Probability Approach to the Examination of Microcracking in Plain Concrete," **Journal of Material Science**, 14: 1141-1151.

Stroeven, P. (1991). "Fractals and Fractography in Concrete Technology," **Brittle Matrix Composites** 3 (Eds A.M. Brandt, I.H. Marshall), Elsevier Appl. Science, London, 1-10.

Stroeven, P. (1992). "Some Mechanical Effects of Interface Debonding in Plain Concrete, Interfaces in Cementitious Composites," **Proceedings**, RILEM Intl. Conf., Ed. J.C. Maso, Toulouse, France, 187–196.

Underwood, E. E. (1968). **Quantitative Stereology**, Addison-Wesley Publishing Company, New Jersey.